

Chromodomain Helicase Binding Protein 8 (Chd8) Is a Novel A-Kinase Anchoring Protein Expressed during Rat Cardiac Development

Maureen O. Shanks¹, Linda M. Lund², Sabrina Manni^{3,4}, Mary Russell⁵, Joseph R. H. Mauban¹, Meredith Bond^{1,6*}

1 Department of Physiology, University of Maryland Baltimore, Baltimore, Maryland, United States of America, **2** Department of Biochemistry, University of Maryland Baltimore, Baltimore, Maryland, United States of America, **3** Department of Medicine, Clinical Immunology and Hematology Branches, University of Padova, Padova, Italy, **4** Venetian Institute of Molecular Medicine (VIMM), Padova, Italy, **5** Department of Biological Sciences, Trumbull Campus, Kent State University, Warren, Ohio, United States of America, **6** College of Sciences and Health Professions, Cleveland State University, Cleveland, Ohio, United States of America

Abstract

A-kinase anchoring proteins (AKAPs) bind the regulatory subunits of protein kinase A (PKA) and localize the holoenzyme to discrete signaling microdomains in multiple subcellular compartments. Despite emerging evidence for a nuclear pool of PKA that rapidly responds to activation of the PKA signaling cascade, only a few AKAPs have been identified that localize to the nucleus. Here we show a PKA-binding domain in the amino terminus of Chd8, and demonstrate subcellular colocalization of Chd8 with RII. RII overlay and immunoprecipitation assays demonstrate binding between Chd8-S and RII α . Binding is abrogated upon dephosphorylation of RII α . By immunofluorescence, we identified nuclear and perinuclear pools of Chd8 in HeLa cells and rat neonatal cardiomyocytes. We also show high levels of Chd8 mRNA in RNA extracted from post-natal rat hearts. These data add Chd8 to the short list of known nuclear AKAPs, and implicate a function for Chd8 in post-natal rat cardiac development.

Citation: Shanks MO, Lund LM, Manni S, Russell M, Mauban JRH, et al. (2012) Chromodomain Helicase Binding Protein 8 (Chd8) Is a Novel A-Kinase Anchoring Protein Expressed during Rat Cardiac Development. PLoS ONE 7(10): e46316. doi:10.1371/journal.pone.0046316

Editor: Kjetil Tasken, University of Oslo, Norway

Received: June 14, 2012; **Accepted:** August 29, 2012; **Published:** October 10, 2012

Copyright: © 2012 Shanks et al. This is an open-access article distributed under the terms of the Creative Commons Attribution License, which permits unrestricted use, distribution, and reproduction in any medium, provided the original author and source are credited.

Funding: Funding provided by NIH F31 AG32162 (PI: Maureen O'Donnell Shanks), NIH R01 AG016613 (PI: Meredith Bond), NIH R01 HL 079134 (PI: Meredith Bond), and NIH T32 HL 072751, "Training Grant in Cardiac and Vascular Cell Biology." The funders had no role in study design, data collection and analysis, decision to publish, or preparation of the manuscript.

Competing Interests: The authors have declared that no competing interests exist.

* E-mail: m.bond40@csuohio.edu

Introduction

Stimulation of G-protein coupled receptors results in elevated amounts of the second messenger molecule cAMP, leading to the activation of protein kinase A (PKA). PKA is a holoenzyme composed of two regulatory (RI or RII) and two catalytic (C) subunits. Activated PKA phosphorylates key substrates (reviewed in [1]). A-kinase anchoring proteins (AKAPs) anchor PKA, by means of its R subunit dimer, to subcellular structures [2], forming microdomains (recently reviewed in [3–5]). This binding confers subcellular localization of PKA, and contributes to PKA specificity and the rapid and effective modulation of PKA-dependent signaling [6].

More than 70 AKAPs have been described to date in multiple cell types and cellular compartments. [1,3,7] Defects in AKAP anchoring or expression have been linked to pathologies such as cardiac arrhythmia [8–11], hypertrophy [12–14], and the progression to heart failure [15,15–18]. Our studies, and those of others, have demonstrated that PKA target phosphorylation is decreased in failing hearts. [15,19,20] The importance of proper PKA signaling in failing myocardium is also linked to transcription, as treatment of patients by use of β -blockers reverses the fetal gene switch between α -myosin heavy chain and β -myosin heavy chain. [21–23] Taken together, the scaffolds formed by AKAPs

represent a powerful mechanism for mediating PKA signaling in the cell, and impaired AKAP:PKA interaction has serious implications for development of cardiac disease.

AKAPs are a functionally diverse family with little sequence similarity, except that they share a characteristic amphipathic α -helical domain that is approximately 14–18 amino acids (aa) in length. [24] This helix has a hydrophobic face that fits in a groove formed by the amino-termini of the R dimer. [24–26] In binding PKA as well as PKA substrates and regulators, AKAPs create a scaffold to effectively localize and modulate signaling through PKA. Given the importance of AKAPs in cardiac function, we used a T7 phage display assay to identify PKA binding proteins. [27] When we screened a cDNA library derived from human heart, we isolated multiple clones of chromodomain helicase binding protein 8 (Chd8), suggesting that Chd8 could also act as an AKAP.

In studies conducted to date, Chd8 has been primarily characterized as a nuclear protein [28] that regulates chromatin dynamics [29–31], transcription [30,32,33], and cell survival [34–36]. Chd8 was first identified as a 749aa nuclear protein named "duplin," [37,38] and found to inhibit the Wnt signaling pathway. [37] In humans, Chd8 predominantly exists in two larger isoforms, Chd8-L1 (2582aa) and Chd8-L2 (2301aa). [29,32,33] (**Figure 1**) Chd8 contains binding sites for and negatively regulates β -catenin

[31,35,37,38] and p53 [36] by means of its ability to bind histone H1. Loss of Chd8 in knockout mice resulted in an embryonic lethal phenotype at embryonic day (E) 8.5 resulting from increased p53-dependent apoptosis. [36,39] Double knockout of Chd8 and p53 extended embryo survival to E10.5, at which point embryos failed to form mesoderm and exhibited massive hemorrhaging characteristic of cardiovascular defects. [36] Chd8 binds other components of transcription, including di-/trimethylated lysine 4 on the histone H3 subunit (H3K4) [30,32,40], RNA polymerase II [32], and members of the Mixed Lineage Leukemia (MLL) complex, WRD5, ASH2L, and RbBP5 [40]. Considering the diversity of its binding partners, Chd8 is likely a component of the scaffold of several large protein complexes, each with a distinct function [40].

Given the evidence for a nuclear microdomain of PKA [41,42], we hypothesized that Chd8 is a novel nuclear AKAP. Also, as Chd8 has largely been studied as a nuclear protein and in the context of development [37–39], we investigated subcellular localization and expression of Chd8 during cardiac development and in non-cardiac cells. Our findings demonstrate a novel localization of Chd8 to a discrete perinuclear microdomain, as well as to the nucleus, and define a new link between PKA-dependent signaling and proteins responsible for chromatin remodeling.

Materials and Methods

Ethics Statement

All animal studies were conducted in compliance with the Animal Welfare Act, Public Health Service Policy on Humane care and Use of Laboratory Animals, and in compliance with the *Guide for the Care and Use of Laboratory Animals*, published by the National Institutes of Health (NIH publication No. 85–23, revised 1996). All animal work was performed under protocols approved by the Institutional Animal Care and Use Committee of the University of Maryland, School of Medicine.

Antibodies, Reagents

Commercial Chd8 antibodies were obtained from Bethyl Laboratories and used for Western blotting and immunoprecipitation (Bethyl Laboratories, Montgomery, TX), and immunofluorescence (Bethyl). Anti-myc-epitope (Cell Signaling Technology, Danvers, Massachusetts), RII α / β (EMD Millipore, Billerica, Massachusetts), RII α (BD, Franklin Lakes, New Jersey), RII β (BD), and anti-Golgi apparatus (EMD) antibodies were used for

western blotting of immunoprecipitates or immunofluorescence, as described. GAPDH (Life Technologies/Ambion, Grand Island, New York) was used for loading control.

Cell Culture

Pregnant Sprague-Dawley female rats were ordered from Harlan Labs (Frederick, Maryland). Primary neonatal cardiomyocytes (NCMs) were harvested from pups at post-natal day 1 and cultured as previously described. [27,43] CHO cells (American Type Culture Collection, Manassas, VA) were cultured in Ham's F12 media with 10% FBS. HeLa cells (ATCC) and HEK cells (ATCC) were cultured in DMEM media (high glucose) with 10% FBS. All transfections were carried out with Lipofectamine-2000 (Life Technologies/Invitrogen).

Plasmids

A plasmid for the 'duplin' isoform of Chd8 (which we refer to as Chd8-S) was kindly provided by Dr Akira Kikuchi, Hiroshima University, Japan. The QuikChange XL Site-Directed Mutagenesis Kit (Agilent/Stratagene, Santa Clara, California) was used to introduce point mutations of key constructs, according to the manufacturer instructions. RII α , RII α -SA, and RII α -SD mutants were created as described [20] and cloned into pEGFP-C1 (Clontech Laboratories, Mountain View, California), in which a CFP was substituted for GFP, for creation of CHO cell lines.

Phage Display Screening

Phage display screening was performed using a human heart cDNA library as previously described. [27] Briefly, a 96-well dish was coated with recombinant RII α purified from *E. coli* expressing RII α -pET11d. 106 clones from a T7-select Phage Display Library (EMD) specific for human heart cDNA were screened. Phage-specific primers were then used for PCR amplification of RII binding peptides, which were sequenced (DNA Sequencing Core Facility, Lerner Research Institute, Cleveland Clinic Foundation) and analyzed with Lasergene software (DNASTAR) and BLAST programs (NCBI, National Institutes of Health). Three clones were isolated and identified by BLASTn search as Chd8.

Western Blotting

For protein extraction of transfected cells, cells were lysed 48 hours after transfection with M-PER Mammalian Protein Extraction Reagent (Thermo Scientific, Rockford, Illinois) with protease inhibitor cocktail (Sigma-Aldrich). NCMs were harvested for protein extraction four days after isolation using a buffer

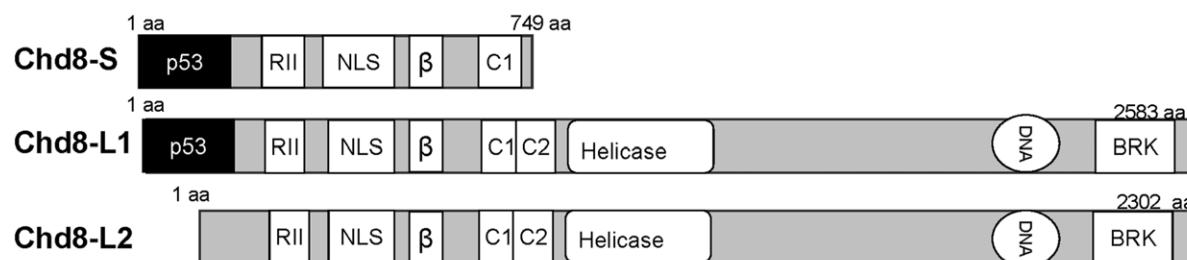


Figure 1. Three isoforms have been identified for Chd8. Chd8-S arises from passage of transcription through the end of exon 9 into intron 10, where it terminates. [32,34] Chd8-S contains a single chromodomain (C1). Two longer isoforms contain the tandem chromodomains (C1 and C2) and helicase domain characteristic to Chd proteins [91,92]. Chd8-L1 and Chd8-L2 result from two different start sites for transcription [32], with the Chd8-L1 transcript encoding an amino terminus extension that encompasses a p53 binding domain [36]. All three isoforms contain a series of five nuclear localization signals (NLS) [38] and a β -catenin binding domain (β) [31,37,39] that is also required for histone H1 [35] binding [35] and STAT3 [28] binding. Chd8-L1 and Chd8-L2 also contain a pair of BRK domains, which mediate chromatin interaction via the histones and is required for interaction with CTCF [29]. All three isoforms contain the AKAP domain (RII) characterized in this study. doi:10.1371/journal.pone.0046316.g001

containing M-PER, 40 mM EDTA, 300 mM NaCl, and protease inhibitor cocktail (Sigma-Aldrich), as described. [27] Micro-BCA was used to determine protein concentration (Thermo Scientific). Lysate was boiled with 4×SDS loading buffer (with DTT), separated by SDS-PAGE, and transferred to PVDF. Western blots used 50 micrograms of total protein per lane, unless noted. The blot was blocked with 5% milk-Tween solution. Blots were incubated with SuperSignal West Pico Chemiluminescent Substrate (Thermo Scientific), and positive bands detected by chemiluminescence. Primary antibodies were used at a dilution of 1:2000, and secondary antibodies at a concentration of 1:10,000, except where otherwise noted in the figure legend.

RII Overlay

PCR primers were used to generate cDNA encoding the RII binding site of rat Chd8 (Chd8^{RII}). This cDNA was cloned into the pTrcHis2/TOPO vector (Invitrogen). Colonies were selected based on antibiotic resistance and sequenced by the Genomics Core Facility (University of Maryland, Baltimore). Bacteria were grown to an OD₆₀₀ value of 0.6, and isopropyl-beta-D-thiogalactopyranoside (IPTG) was added to induce expression according to manufacturer's instructions. A control vector containing LacZ was transformed and used to verify expression. Samples were taken hourly, prepared with 1× Laemli loading buffer with β-mercaptoethanol, separated by electrophoresis and transferred to nitrocellulose for Western blotting. For RIIα overlays, 5 mL of bacterial culture suspended in LB was collected at hour 3, spun down, and lysed in 1× SDS loading buffer. Bacterial lysate separated on a 12% Tris-HCl gel and transferred to nitrocellulose membrane. The control expression protein (LacZ) as a negative control. Purified recombinant RIIα (5 μg/mL in 10% BSA/TBS), was incubated alone, or with either 50 μM Ht31 or Ht31P peptides (generated by Biopolymer Core, University of Maryland, Baltimore). After blocking for 1 hour, separate blots were incubated overnight with the RIIα solutions. Each blot was washed thoroughly and developed using antibody against RIIα/β (EMD).

Co-immunoprecipitation

Immunoprecipitations of tagged protein constructs were conducted with the myc-tag co-immunoprecipitation kit (Thermo Scientific) according to manufacturer's instructions.

Immunostaining and Inverted Fluorescent Microscopy

Cells were grown on glass coverslips and fixed with 4% paraformaldehyde in PBS for 10 minutes at room temperature, then permeabilized with 0.1% Triton X/PBS for 10 minutes. Cells were blocked with 3% BSA/PBS, and then incubated with primary antibody at the following dilutions: myc antibody (CST, 1:250), Chd8 (Bethyl, 1:200 or 1:50), RIIα/β (EMD, 1:80), Golgi apparatus (EMD, 1:100), α-actinin (Sigma-Aldrich, 1:250). For Figure S4, cells were immunolabeled with Chd8-Sigma, a polyclonal antibody purified from anti-sera from New Zealand White rabbits inoculated with 77–90aa of Chd8 (Sigma-Aldrich Genosys, St Louis, Missouri). Sera was purified, eluted from the purification column, and used for immunofluorescence at a dilution of 1:250 (HeLa) or 1:150 (primary rat neonatal cardiac cells). Cells were washed for 1 hour with 1% BSA/PBS, incubated with Alexafluor conjugated antibodies (Life Technologies/Invitrogen, Grand Island, New York) as indicated at 1:500, and washed again. Coverslips were mounted and nuclei were stained using Vectashield mounting medium with DAPI (Vector Laboratories, Burlingame, California). All antibody incubations occurred for 1 hour at room temperature, except for myc and Chd8-Sigma,

which occurred at 4°C overnight. Immunostaining was visualized with a Nikon TE2000-U inverted fluorescent microscope (Nikon Instruments, Melville, New York) and images were obtained with a Spot digital camera (Diagnostic Instruments, Inc., Sterling Heights, Michigan) with Spot Advanced 4.0.2 software.

Confocal Microscopy

A Zeiss 5 Live slit scanning confocal microscope was used to image HeLa cells that were colabeled with antibodies for Golgi apparatus and Chd8. Imaging was performed with a 63X, 1.4 NA oil immersion objective, and data acquisition was set at .21 μm/pixel, 12 bit. The Alexafluor goat anti-mouse 568 antibody used to detect Golgi signal was excited at 561 nm and emission was long pass filtered at 575 nm. Excitation of Chd8 signal, detected by Alexafluor goat anti-rabbit 488 was at 489 nm and emission was bandpass filtered at 495–555 nm.

Taqman Quantitative PCR and Analysis

Rat hearts were harvested for RNA extraction with the Quick Prep Total RNA Extraction kit (GE Life Sciences, Piscataway, New Jersey) at embryonic days (16 and 19), post natal days (1, 3, 7, and 21), and six months. RNA was converted into cDNA with the iScript kit (Bio-Rad, Hercules, California). 20 ng of cDNA was used per assay. Taqman probes for Chd8 (Rn00576005_m1, designated Probe 1, and Rn01414467_m1, designated Probe 2), RIIα (Rn00709403_m1), and GAPDH (Rn 99999916_s1) were obtained from Applied Biosystems, and used in conjunction with Master Mix (Applied Biosystems, Carlsbad, California) as described for PCR amplification with a 7900HT Thermal Cycler (Applied Biosystems), as described. [44] Each sample was assayed in triplicate, and the average of the three values was normalized to GAPDH (internal reference). Relative quantitation of mRNA was calculated using 2^{-ΔΔCt} method, as described elsewhere [45], with embryonic day 16 set to “1”.

Results

Identification of Chd8 as a Novel Binding Partner for RIIα

The T7 phage display assay was used to screen a human heart cDNA expression library to identify novel cardiac AKAPs. This approach identified several known RIIα binding proteins that served as positive controls and verified our method. These included RIIα [46] and two known cardiac AKAPs, mAKAP [47] and AKAP-Lbc [12,48]. We isolated clones that contained fragments of seven previously unidentified RIIα binding proteins. One of those proteins, synemin, is an intermediate filament protein that we characterized as a novel AKAP that associates with the Z-discs and cell junctions in cardiac myocytes [27,44].

Among the proteins we identified as binding partners for RII, three clones contained peptide fragments of Chd8. Using BLAST analysis of the peptide fragments, we found that the three clones overlapped with the amino terminus of Chd8 and encoded 391–545aa of the Chd8-L1 isoform. This sequence is present in all three isoforms of Chd8 and is located immediately upstream of a nuclear localization signal (NLS). (**Figure 1**) Because of the known role for Chd8 in regulating transcription and cell survival, we focused our investigations on the potential role of Chd8 as an AKAP.

Given the importance of an amphipathic α-helix to the RII:AKAP interaction [24], we used bioinformatics to analyze the predicted secondary structure of Chd8 to identify putative amphipathic helices. We translated the Chd8 cDNA and used this amino acid sequence to predict regions of α-helical domains within the Chd8 sequence. (**Figure 2A**) A search was conducted using

GeneiousPro, a bioinformatic platform that includes a tool for generating secondary structure predictions via the EMBOSS Garnier algorithm. [49,50] A second tool, JPRED, predicts secondary structure and utilizes position-specific scoring matrices, Hidden Markov Model profiles, and structures stored in databases like UniProt and PDB to predict protein structure and accessibility of amino acid residues. [51] Both algorithms predicted an α -helix within the Chd8 peptide that was isolated by the phage display, generating a targeted prediction of an AKAP domain. (**Figure 2A, 2B**).

A ClustalW alignment [52] was performed with the Chd8 fragment and the RII binding domains of several known AKAPs. (**Figure 2C**) The AKAP domains aligned with amino acids within the Chd8 α -helix (455–473aa of Chd8-L1). Hydrophobic profiles of aligned sequences were also similar. (**Figure 2C**) A two dimensional helical wheel plot was generated of the proposed Chd8 RII α binding site (KKQEKANRIVAEAIARAR). The 2D plot shows clustering of hydrophobic residues on one side of the helix, consistent with RII binding domains of other AKAPs. [53] (**Figure 2D**) This region of the Chd8 sequence is very highly conserved across species. (**Figure 2E**) Thus, using a large scale screening method in conjunction with bioinformatics-based approaches, we identified an amphipathic α -helical structure within the Chd8 peptide fragment that associated with RII α in our phage display assay. This α -helical region displayed similar amino acid properties as other known AKAPs.

Chd8 Binds to RII α *in vitro*

RII overlay was used next to determine the binding capability of RII α to this fragment of Chd8. RII overlay is frequently used to identify novel PKA binding proteins [46,54] and exploits the ability of RII to bind AKAP protein on a Western blot. We cloned a 150 amino acid fragment of Chd8 (Chd8^{RII}, corresponding to 390–530aa of Chd8-L1). This peptide was then expressed as an inducible His/myc fusion protein in *E. coli*. (**Figure 3A**) Mutation of a hydrophobic residue within the amino acid sequence of an AKAP to a Pro residue is sufficient to abolish α -helical structure and disrupt PKA binding [25,55,56]; therefore we used site-directed mutagenesis to introduce a Pro mutation at Ile 464 (Chd8^{RII}-P). Based on the bioinformatics analysis of the predicted RII α binding domain, we predicted that this mutation would eliminate RII α binding. Immunoblotting methods were used to demonstrate expression of each construct (~22 kDa MW). (**Figure 3B**).

In RII overlay assays, purified recombinant RII α bound to a 22 kDa band in protein extracted from bacteria expressing Chd8^{RII}, indicative of a 22 kDa RII α binding protein. (**Figure 3C**, top, center lane) In contrast, no corresponding bound RII α was detected in lysate from bacteria expressing Chd8^{RII}-P, indicating a loss of RII α binding ability in the fragment carrying the I464P mutation. We then pre-incubated RII α with Ht31 or Ht31P. Ht31 is a peptide derived from the AKAP domain of AKAP-Lbc that is commonly used to inhibit AKAP:PKA

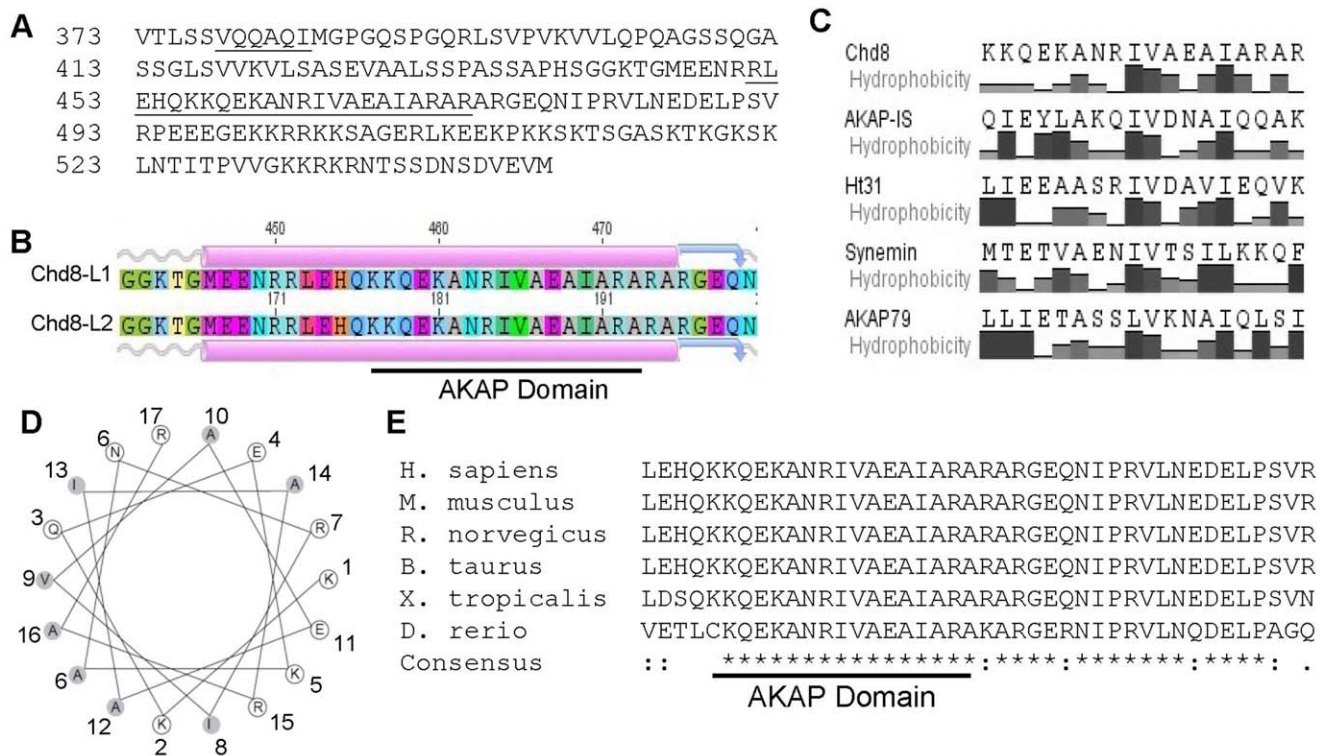


Figure 2. Bioinformatics analysis of Chd8 reveals a predicted α -helix. Bioinformatics analyses of the Chd8 peptide identified in T7 phage display with JPRED2 (A) and Geneious (B) bioinformatics tools show predicted α -helices within the amino acid sequence. C) ClustalW alignment of Chd8 with known AKAP domains. Hydrophobicity plots for each peptide are listed below the amino acid sequence. D) A 2D helical wheel plot was generated for the predicted AKAP domain of Chd8. Hydrophobic amino acids are shaded in gray, and amino acids are numbered starting from the amino terminus. E) Alignment of the predicted AKAP domain (underlined) in Chd8 shows a high level of conservation between species. Sequences from *H. sapiens* (NP_001164100.1), *M. musculus* (NP_963999.2), *R. norvegicus* (NP_075222.2), *B. taurus* (NP_001179063.1), *X. tropicalis* (NP_001131089.2), and *D. rerio* (NP_001189381.1) were used. An asterisk (*) denotes a conserved amino acid, a colon (:) denotes strongly similar amino acids, and a period (.) denotes weakly similar amino acids. doi:10.1371/journal.pone.0046316.g002

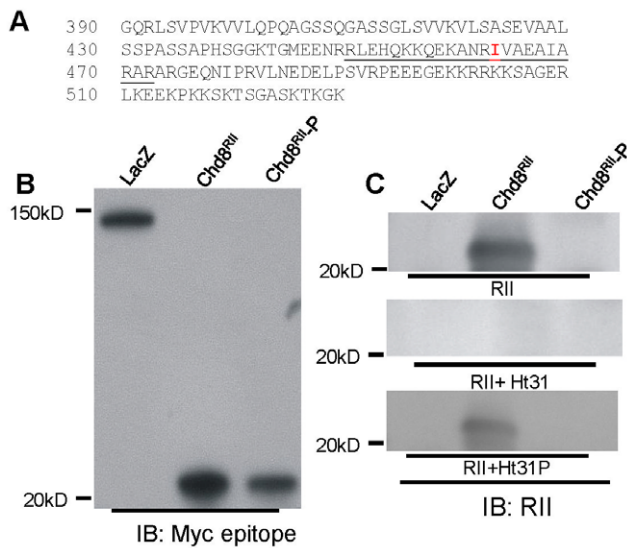


Figure 3. RII α binds to Chd8^{RII} in RII overlay, but not to Chd8^{RII-P}. **A**) PCR amplification of rat Chd8-S generated a construct with the predicted protein sequence of Chd8, as well as a c-terminal myc tag (not shown). The AKAP domain is underlined. Site-directed mutagenesis was used to mutate I464 (red) to a Pro for the Chd8^{RII-P} construct. **B**) Expression of constructs following induction with IPTG. Constructs were expressed in *E. coli* and grown to log phase before the addition of IPTG to induce expression. As a control for induction of protein, a myc-tagged LacZ construct was used (left lane, 140 kDa MW). Chd8^{RII} (second lane) and Chd8^{RII-P} (third lane) were expressed at the predicted molecular weight of approximately 22 kDa. **C**) RII α overlay was conducted with Western blots of *E. coli* lysate from bacteria expressing inducible constructs. *Top*: In membranes incubated with RII α , RII α / β antibody detected bound RII α to the lane expressing Chd8^{RII}, but not to the lane expressing Chd8^{RII-P}. *Middle*: Pre-incubation of RII α with Ht31, an inhibitor of RII:AKAP interaction, resulted in loss of binding to Chd8^{RII}. *Bottom*: Pre-incubation of RII α with Ht31P, a prolated form of Ht31 unable to bind RII, did not prevent binding of RII α to protein in the Chd8^{RII} lane. No corresponding bands were observed in the negative control (LacZ) lanes.

doi:10.1371/journal.pone.0046316.g003

interaction and Ht31P is the same peptide containing a Pro mutation that disrupts the structure of the AKAP domain and prevents association of the peptide with the RII dimer. [24,25,57,58] Pre-incubation of RII α with Ht31 peptide prevented the binding of RII α to Chd8^{RII} in RII overlay, whereas the pre-incubation of RII α with Ht31P had no effect. (**Figure 3C**, center and bottom) We concluded that, like other known AKAPs, RII α binds Chd8^{RII}, but not Chd8^{RII-P}, in RII overlay assays.

We then investigated whether Chd8 and RII α interact in intact cells. CHO cells were transfected with either Chd8-S or Chd8-S-P, the latter of which contained the same I464P mutation that was sufficient to prevent binding of RII α to Chd8^{RII-P} in the RII overlay assays. Immunofluorescence and Western blotting methods showed that the I464P mutation did not interfere with localization or expression of myc-tagged Chd8-S. (**Figure 4A, 4B**) CHO cells were cotransfected with RII α and with either Chd8-S or Chd8-S-P. RII α co-immunoprecipitated with Chd8-S, but not with Chd8-S-P, demonstrating that the I464P mutation in the AKAP domain of Chd8-S resulted in loss of binding to RII α . (**Figure 4C**) No RII α was detected in immunoprecipitation of single transfections. We concluded that Chd8-S and RII α coimmunoprecipitate when coexpressed in CHO cells, but that mutation of the RII α binding domain in Chd8-S leads to loss of interaction. As I464P was sufficient to prevent coimmunoprecipitation

of Chd8-S and RII α , we also concluded that the RII α binding domain which we identified by bioinformatics and RII α overlay is the only RII α binding domain in Chd8-S.

As experimental and modeling evidence has defined a nuclear microdomain of AKAP-bound PKA in the nuclei of HEK cells [41], we used cAMP-coupled agarose beads to pull down cAMP-binding proteins in HEK cell lysate. RII α and RII β were detected in proteins that eluted with cAMP agarose. Addition of 8-Br-cAMP, a non-hydrolyzable analogue of cAMP, competed with the cAMP agarose for cAMP binding and reduced the amount of RII α and RII β pulled down by the beads. A high molecular weight band corresponding with Chd8-L1 was also detected in pull-down assays with cAMP beads, but not in samples incubated with 8-Br-cAMP. (**Figure 5**) We concluded that Chd8 co-elutes with the cAMP-binding proteins RII α and RII β .

Phosphorylation of RII α at Serine 96 Inhibits PKA Anchoring by Chd8-S

Autophosphorylation of RII α by the C subunit at a Ser (Ser96) in the inhibitory domain of RII α promotes the activation of C for target phosphorylation. [59–61] Our recent findings demonstrate that dephosphorylation of Ser96 promotes reassembly of the PKA holoenzyme and reduces binding of RII α to AKAP15/18. [19,20] Thus, autophosphorylation of RII α at Ser96 plays a key role in modulation of PKA activity and localization of the holoenzyme. We next investigated whether RII α regulation via autophosphorylation affects the interaction between Chd8-S and RII α .

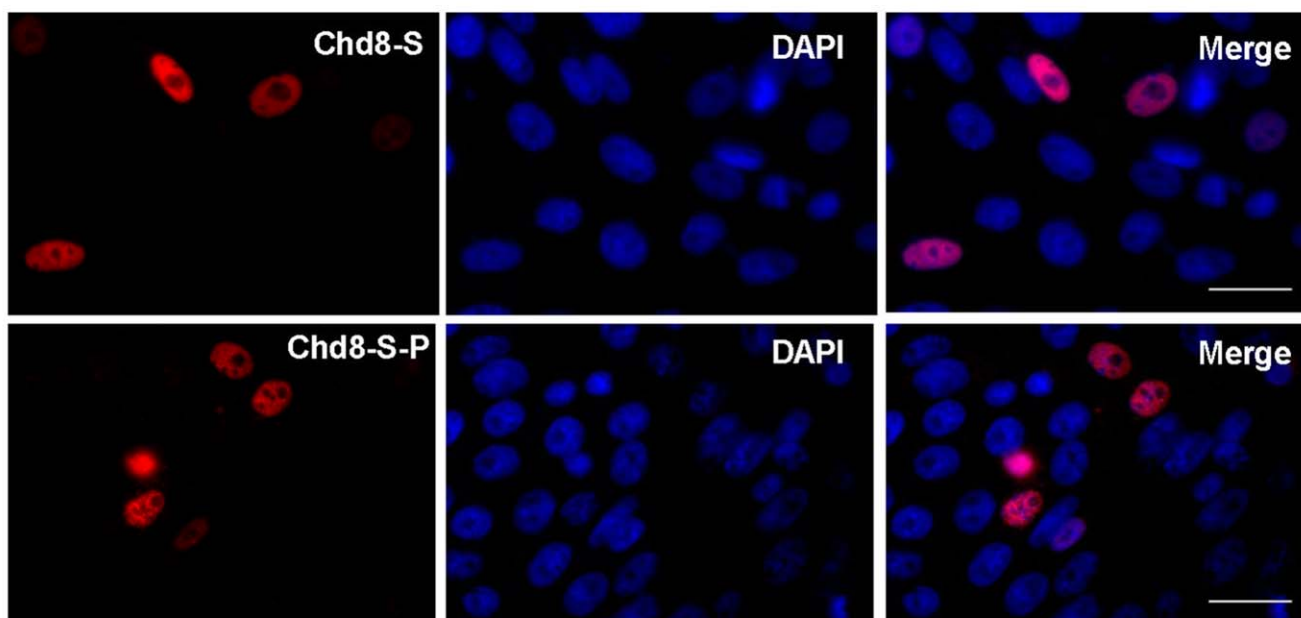
We created three CHO cell lines stably expressing RII α constructs in which Ser96 was not altered (RII), or was mutated to Ala, in order to mimic constitutively dephosphorylated RII α (RII-SA). RIIa was also mutated to Asp to mimic constitutively phosphorylated RII α (RII-SD). Expression of each RII α construct was verified by immunofluorescence, using a CFP tag (**Figure 6A**), and by Western blot analysis (**Figure 6B**). Each cell line was transiently transfected with Chd8-S. (**Figure 6B**) Chd8-S was immunoprecipitated from all transfected cultures. Western blot analysis of the Chd8-S immunoprecipitate identified RII and RII-SD, but not RII-SA. (**Figure 6C**) As this result was consistent with the anchoring dynamics of other AKAPs [19,20], we concluded that dephosphorylation of Ser96 (RII-SA) eliminates the interaction of RII α and Chd8-S, whereas autophosphorylation of RII α at Ser96 promotes binding of Chd8 and RII α .

Subcellular Localization of RII and Chd8

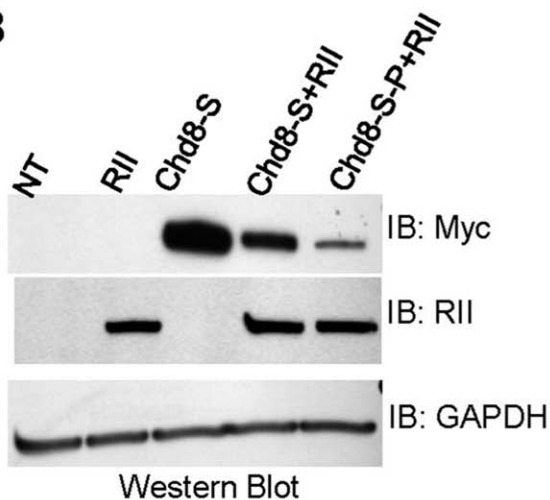
Consistent with the first study of Chd8-S [37,38], our localization studies of cells overexpressing the Chd8-S isoform show that it is restricted to the nucleus (**Figure 4A**). [37,38] However, since those studies were published, additional isoforms of Chd8 (Chd8-L1 and Chd8-L2) have been described. Other AKAP genes, including those for AKAP350 [62] and AKAP-Lbc [63,64] encode multiple isoforms with different patterns of subcellular localization. To determine if the longer Chd8 isoforms exhibit the same subcellular localization pattern, we examined the endogenous localization of Chd8.

We immunostained HeLa human adenocarcinoma cells, which have been previously used to identify Chd8 binding partners [31], with a polyclonal antibody raised against a 50 amino acid fragment of the carboxy terminus of Chd8-L1 and Chd8-L2. Our immunostaining of endogenous Chd8 revealed nuclear staining (**Figure 7A**, arrowhead; Figure S2A), but, interestingly, we also found a perinuclear pattern of immunofluorescence. (**Figure 7A**, arrows) This staining pattern was reproduced using an alternate antibody raised against the amino terminus of Chd8. (Figure S4A) Because of the distinctive perinuclear pattern, we costained HeLa

A



B



C

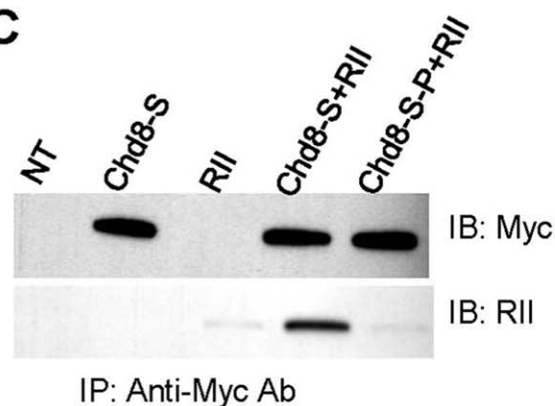


Figure 4. RII α co-immunoprecipitates with Chd8-S, but not Chd8-S-P. A) Immunofluorescence of transfected cells shows nuclear localization of Chd8-S and Chd8-S-P constructs (red). Cells were imaged with inverted fluorescent microscopy at a magnification of 90X. Scale bar represents 25 μ m. B) Western blot analysis of protein extracted from CHO cells transfected with Chd8-S, RII α , or a combination of Chd8-S and RII α or Chd8-S-P and RII α . Chd8 constructs were detected by means of an antibody to a myc epitope tag. RII α constructs were detected with a pan-RII antibody. GAPDH was used as a loading control. C) Cell lysate for single and co-transfections was subject to immunoprecipitation for myc-tagged constructs. In the single transfection of Chd8-S, immunoprecipitation with antibodies to the myc tag isolated Chd8-S. No product was observed in the single transfection with RII α . For co-transfections, immunoblotting showed immunoprecipitation of RII α with Chd8-S, but not Chd8-S-P. No target proteins were identified in immunoprecipitate from untransfected cells (NT). (n = 3, representative blots shown). doi:10.1371/journal.pone.0046316.g004

cells with an antibody raised against the Golgi fraction of human cells. We observed perinuclear immune-labeling of Chd8 in the region of the Golgi apparatus. (**Figure 7A**) Confocal microscopy of HeLa cells co-labeled with antibodies raised against Chd8 and Golgi showed similar plot profiles of the immunofluorescence patterns in the same focal plane. (**Figure 7B**) Addition of the immunogen against which the Chd8 immunostaining antibody was raised resulted in loss of both the nuclear and perinuclear immune-labeling. (Figure S2) Costaining of HeLa cells with

antibodies against Chd8 and PKA RII α / β demonstrated perinuclear staining for both proteins. Overlay of images demonstrated subcellular colocalization of these signals, particularly in the perinuclear domain. (**Figure 7C**, arrows).

Chd8 is Expressed in Rat Cardiac Development

Chd8 was isolated in our screen for novel cardiac AKAPs. [27] As Chd8 has been implicated in embryonic development

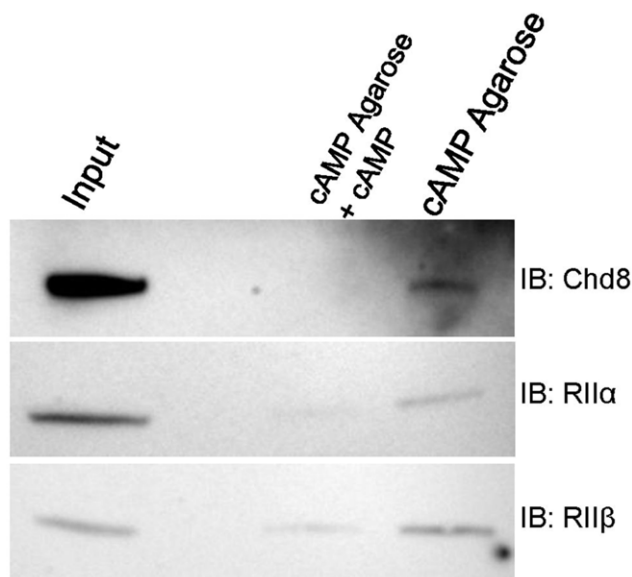


Figure 5. Chd8 is detected with RII subunits in cAMP-pull down. Protein extracted from HEK 293T cells was used for pull-down with cAMP-coupled agarose. Bound proteins were eluted and analyzed by Western blot. *Top:* Chd8 was detected in input lane (left lane) and with eluate from cAMP agarose. The cAMP analogue 8-Br-cAMP was used as a negative control, to compete binding to the cAMP-agarose. Chd8 was not detected in the negative control lane. *Middle:* Detection of RII α with an RII α monoclonal antibody showed RII α in the input lane and the cAMP-agarose lane. *Bottom:* Detection of RII β with an RII β monoclonal antibody showed RII β in the input lane and cAMP-agarose lane. Addition of cAMP reduced, but did not entirely eliminate, pull-down of RII α and RII β in this experiment. (n=3, representative blots shown). doi:10.1371/journal.pone.0046316.g005

[36,37,39], we examined the expression of Chd8 in developing rat cardiac tissue. In a study of mouse embryos, Chd8 mRNA is expressed at high levels early in embryogenesis and lower levels found in adult mice. [37,39] Given Chd8's role as a negative regulator of p53, differential regulation of Chd8 may contribute to p53-dependent apoptosis required in organogenesis [36], or to the selective regulation of the Wnt/ β -catenin pathway during development [31,35].

Two sets of Taqman probes were used to detect Chd8 mRNA in developing cardiac muscle. (**Figure 8A**) Probe 1, which spans exons 2–3 and encompasses the AKAP binding domain of Chd8, recognizes all three isoforms transcripts of Chd8. Probe 2 recognizes Chd8-L1 and Chd8-L2 and spans exons 12 and 13, which encode the helicase domain. A probe against the mRNA transcript for RII α (PKAR2A) was used to measure RII α mRNA. We detected high levels of cardiac CHD8 mRNA at PN7, followed by a decrease to low but detectable levels in 6 month-old rat heart. (**Figure 8B**).

We next utilized rat neonatal cardiac myocytes to study expression of Chd8 protein in the heart. Western blot analysis of myocyte protein extract identified both the Chd8-L1 and Chd8-L2 isoforms. (**Figure 8C**) Immunofluorescence of fixed cultures showed Chd8 expression in both myocytes (**Figure 8D**, arrows) and fibroblasts (**Figure 8E**, arrowheads). As we previously reported above for HeLa cells, the antibody to Chd8 detected nuclear immunostaining, as well as a perinuclear pool of Chd8, in both cell types. (**Figure 8D**) This staining pattern was reproduced using an alternate antibody raised against the amino terminus of Chd8. (Figure S4B) In contrast, we observed only perinuclear

staining of RII α / β in myocytes and fibroblasts. (**Figure 8E**) These findings indicated that Chd8 is expressed in cardiac cells, where it localizes to both nuclear and perinuclear domains, similar to the immunostaining pattern seen in HeLa cells. (Figure S2B).

Discussion

We have shown that Chd8, previously identified as a chromatin binding protein, also binds RII α in intact cells and is thus a new member of the AKAP family. Similar to our previous findings that phosphorylated RII α has a higher affinity for AKAPs than dephosphorylated RII α [19,20], we demonstrated that phosphorylation of RII α is required for Chd8:PKA association. Furthermore, in addition to the identified nuclear localization of Chd8, we also demonstrated a novel perinuclear localization of Chd8 in close proximity to the Golgi apparatus.

Chd8 Contains an AKAP Domain in its Amino Terminus

Having established RII α binding to Chd8 by phage display, we used bioinformatics, including the prediction of secondary structure, predictive modeling, alignments, to identify the AKAP domain of Chd8. (**Figure 2**) Bioinformatics has been previously used to study R:AKAP interactions, and is a powerful tool when paired with experimental approaches. [58,65,66] A study by McLaughlin *et al.*, published while this manuscript was in progress, also identified a 24 amino acid peptide of Chd8 that overlaps with the Chd8 PKA binding domain. This domain was identified using our own bioinformatics-based approach. McLaughlin *et al.* used a panel of Ala mutations within the Sphingosine kinase interacting protein (SKIP) to show that SKIP is a dual AKAP. [65] In contrast, another recent study used molecular modeling together with site-directed mutagenesis and immunoprecipitation, to show that SKIP is exclusively an RI-specific AKAP that does not bind RII. [66] These divergent findings highlight the importance of pairing experimental manipulation with bioinformatics approaches.

Our findings that dephosphorylation of RII α at Ser96 prevents the binding of Chd8 and RII α suggest a mechanism by which anchoring of PKA to Chd8 may be regulated within nuclear and/or perinuclear microdomains. (**Figure 5**) RII α phosphorylation at different sites modulates the affinity of the RII α dimer for AKAPs within the same subcellular compartment. [10,67] Our previous work shows that PKA autophosphorylation of RII α in the inhibitory domain at Ser96 increases the affinity of RII α for AKAP15/18. [20] Past work from our lab also demonstrated that the relative decrease in affinity of RII α for AKAPs upon dephosphorylation at Ser96 varies between AKAPs. For example, the decrease in binding affinity between dephosphorylated RII α and AKAP15/18 is more than 600 times greater than the decrease in binding affinity for dephosphorylated RII α and AKAP-Lbc, as compared to phosphorylated RII α . [16,19] Our studies likewise demonstrate that phosphorylation of RII α at Ser96 increases the probability of RII α association with Chd8. In unstimulated cells, low levels of RII α phosphorylation have been observed, under baseline conditions, and exogenously expressed RII α can be phosphorylated and dephosphorylated at Ser96. [20] Since we observed immunoprecipitation of Chd8-S with RII-SD but not RII-SA, it is likely that the RII α that is immunoprecipitated in our assay is phosphorylated. We also observed a perinuclear distribution of RII and RII-SD. (**Figure 6B**, arrows) We hypothesize that phosphorylation of RII α at Ser96 may serve as a molecular switch that increases binding affinity for Chd8 versus RIIa binding to other AKAPs in the same compartment.

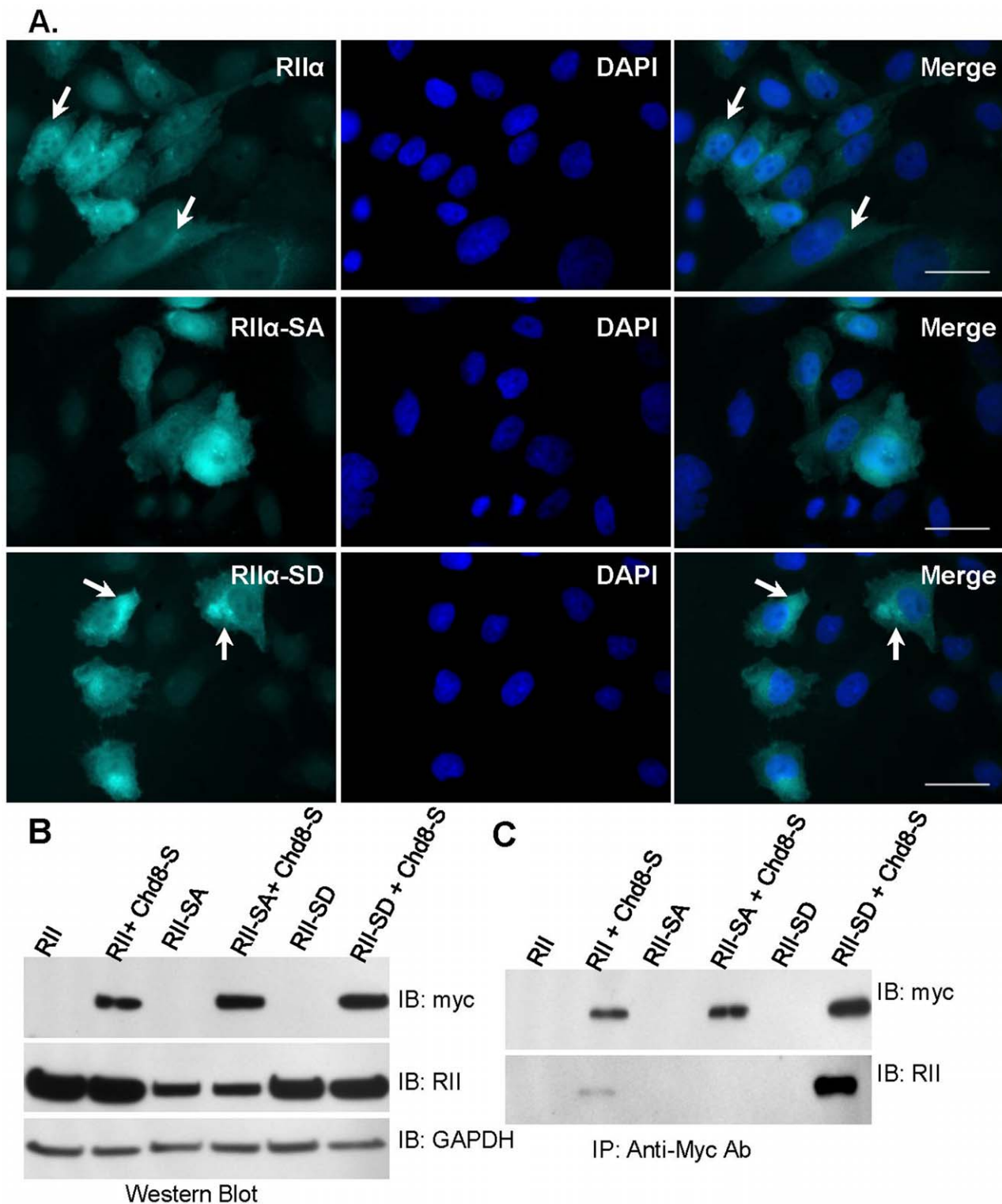


Figure 6. Chd8-S coimmunoprecipitates with RII α and RII α -SD, but not RII α -SA. A) RII α , RII α -SA, and RII α -SD constructs were stably expressed in CHO cells and visualized through a carboxyl CFP tag. Arrows point to a punctate distribution of the RII α constructs observed in RII α and RII α -SD cell lines. Cells were imaged with inverted fluorescence microscopy and images taken at 90X magnification. Scale bar represents 25 μ m. B) Western blot analysis of CHO cells stably expressing RII α , RII α -SA, or RII α -SD alone, or transiently transfected with myc-tagged Chd8-S. Chd8 constructs were detected by means of an antibody to a myc epitope tag. RII α constructs were detected with a pan-RII antibody. GAPDH was used as a loading control. C) CHO cell lysate was subject to immunoprecipitation with antibodies to the myc tag of Chd8-S. In co-transfected lanes, immunoblot of immunoprecipitate detected RII α -SD and RII α in immunoprecipitates of Chd8-S, but not RII α -SA. No target proteins were detected in the CHO cell lysates expressing RII α constructs alone. (n=3, representative blots shown). doi:10.1371/journal.pone.0046316.g006

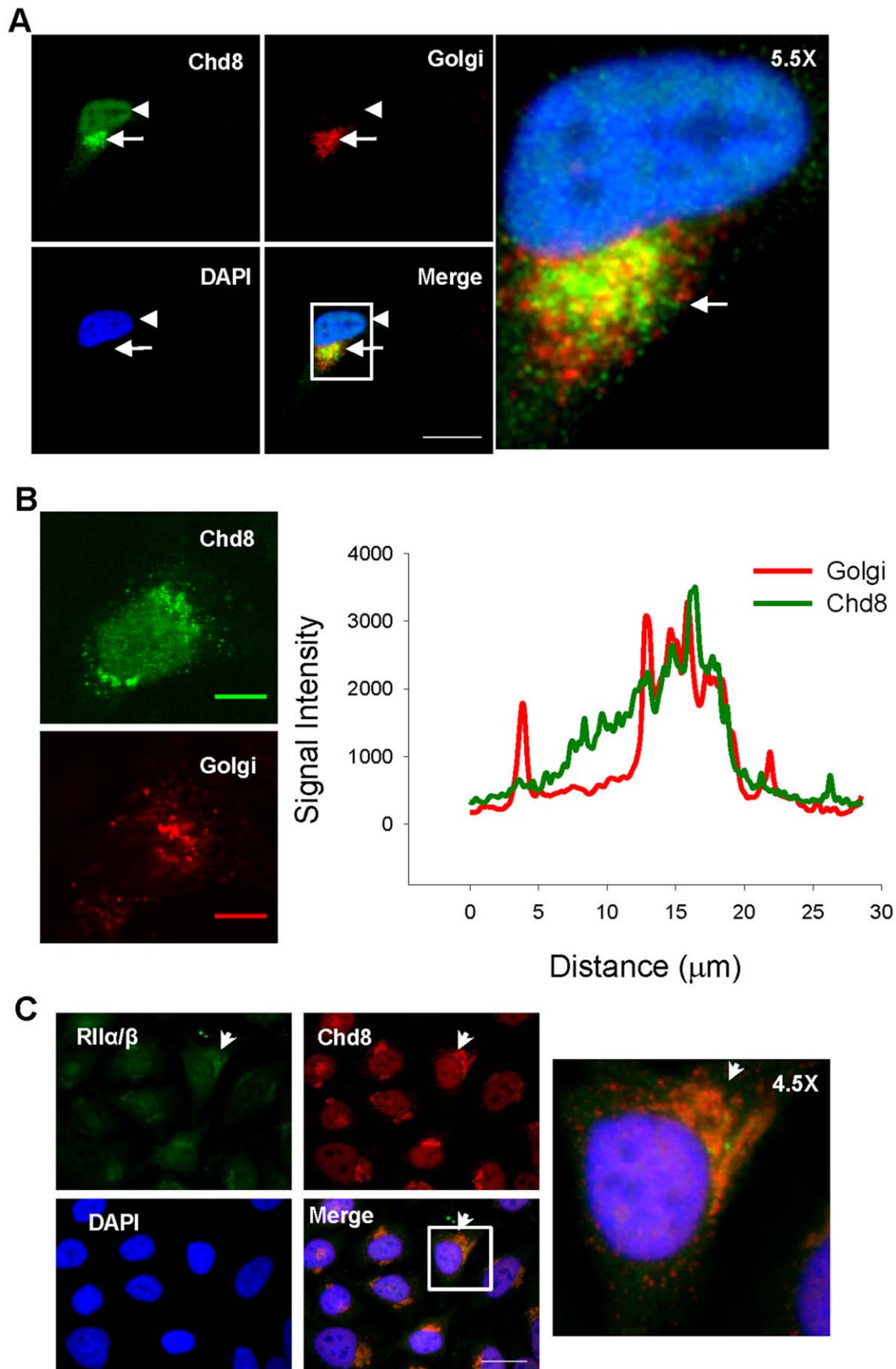


Figure 7. Subcellular localization of Chd8 and RII α / β in HeLa cells. A) Immunofluorescence of endogenous Chd8 (green) identified nuclear Chd8, and also a discrete perinuclear staining (arrow, arrowhead). Immunofluorescence of the Golgi apparatus (red) with an antibody to human Golgi reveals distinct perinuclear localization. Merge shows that the perinuclear pool of Chd8 is in close proximity (arrowhead) to or overlapping with (arrow) the Golgi apparatus. Inset shows cell that was magnified 5.5 \times for the right panel. Cells were imaged with inverted fluorescence microscopy and images taken at 90 \times magnification. Scale bar represents 25 μ m. B) Confocal microscopy of Chd8 (green) and Golgi (red) immunofluorescence in the same transverse slice. The graph represents the plot profile for signals across each channel in the same plane. Images taken at 63 \times magnification, the scale bar represents 10 μ m. C) Costaining for RII (green) and Chd8 (red) in HeLa cells. The merge reveals overlapping signals between RII and Chd8 in the perinuclear staining (arrows). Inset shows cell that was magnified 4.5 \times for the right panel. Cells were imaged with inverted fluorescence microscopy and images taken at 90 \times magnification. Scale bar represents 25 μ m.
doi:10.1371/journal.pone.0046316.g007

AKAPs target other proteins that regulate stability of cAMP and the phosphorylation state of R. [68] Based on our findings, we propose that Chd8 anchors PKA in close proximity to p53, histone H1, or β -catenin in the nucleus following activation of the PKA signaling pathway. (**Figure 1**) Other AKAPs bind phosphodiesterases or protein phosphatases, which attenuate the PKA pathway after the elevation of cAMP. [3,68] Recent work characterizing a nuclear PKA microdomain identified candidate binding proteins for nuclear AKAPs, including soluble adenylyl cyclase (AC). Soluble AC could participate in nuclear PKA signaling. [42,69] One intriguing result arose from modeling the activation of a nuclear microdomain of cAMP and PKA. [41] This study reported a nuclear microdomain of PKA that permitted rapid activation kinetics of PKA in the nucleus following activation of sAC. Introduction of a hypothetical nuclear AKAP into this kinetic model likewise implicated the importance of PKA and phosphodiesterase anchoring in the nucleus, although no specific AKAP was manipulated experimentally. [41] Chd8 is a possible candidate for this unknown AKAP.

Chd8 Exists within Nuclear and Perinuclear Microdomains

Few AKAPs have been reported to reside in the nucleus. Despite a longstanding model in which C subunits of PKA translocate to the nucleus following elevation of cAMP, several reports indicate that a nuclear microdomain of PKA [41,42,70–73] and cAMP [42,69,74] does exist, possibly governed by sAC. [41,42,69,75] The nuclear distribution of PKA regulatory subunits has been reported in multiple cell lines and tissues [41,70,72,73,76–79], including HeLa cells [42]. Localization of AKAPs to the nucleus permits rapid and effective signal transduction in the nuclear compartment. [41] To date, nuclear AKAP95 has been best characterized: PKA anchoring via AKAP95 is required for proper chromatin condensation during mitosis. [67,80–82] AKAP7 [83] and nAKAP150 [76] localize to the nucleus during development, whereas the splicing factor SFRS17A is a dual AKAP that regulates pre-mRNA splicing. [84] Our identification of an AKAP domain in Chd8 expands the understanding of the roles of nuclear AKAPs.

Some AKAPs, e.g. AKAP350, AKAP13, exhibit alternative subcellular localization of different isoforms. [62–64] Our results indicate that Chd8 exists in at least two microdomains, one nuclear and one perinuclear. (**Figure 7**) It remains to be determined if the two pools of Chd8 contain different isoforms, or if Chd8-L1 and Chd8-L2 are present in both. Given the functional diversity of AKAPs, isoforms of Chd8 may play differential role in anchoring PKA to different subcellular microdomains.

Similar to its subcellular distribution in HeLa cells, we showed that Chd8 exhibits nuclear and perinuclear localization in cardiac cells. (**Figure 8D**) The distribution of the perinuclear immunostaining in cardiac myocytes differed from the distribution in fibroblasts. Interestingly, in myocytes, connexin-43, which is trafficked from the Golgi apparatus to cell junctions by anterograde vesicular transport, exhibits a similar compact perinuclear

immunostaining pattern, attributed to its localization in the Golgi. [85] The similarity of staining patterns suggests colocalization of perinuclear Chd8 with the Golgi apparatus in myocytes. Our immunostaining of RII in myocytes did not show detectable RII in the nuclei of myocytes or cardiac fibroblasts. (**Figure 8E**) As analysis of mouse heart protein has shown expression of all four isoforms of R subunit [86], it is possible that nuclear localization of R varies between cell types, or that rat heart expresses PKA isoforms in a different pattern than in murine cardiac tissue. Alternatively, the nuclear microdomain of PKA may be more easily detectable in other cell lines. HeLa cells, among other cell types, have been shown to contain nuclear PKA holoenzyme. [41,42,78] Thus, Chd8 may act as an AKAP in the nucleus and in the perinuclear domain of HeLa cells, whereas in cardiac myocytes, PKA anchoring by Chd8 may be restricted to the perinuclear domain.

The mechanism by which Chd8 localizes to the perinuclear region remains to be determined. The phosphorylation of residues within an NLS is one mechanism to regulate nuclear localization of a protein. [87] Analysis of the Chd8 NLS with PKAPs, a program designed to predict PKA phosphorylation sites, identifies several potential PKA targets in the Chd8 NLS. [88] (Table S1) Given the close proximity of anchored PKA to the NLS, one function of anchored PKA may be the phosphorylation of Chd8 itself.

Chd8 is Expressed at High Levels in Post-natal Heart

We demonstrated that Chd8 is expressed during embryonic and post-natal cardiac development and also in myocytes and fibroblasts from post-natal rat hearts. (**Figure 8**) Previous reports described peak levels of Chd8 mRNA in whole mouse embryos, with a decline of Chd8 mRNA in newborn mice. [37] In contrast, our results indicate that, in rat heart, a high level of Chd8 mRNA is detected for at least a week after birth. To date, Chd8, a regulator of cell cycle genes and apoptosis, has been studied in cancer cell lines and in vascular smooth muscle cells, capable of division in culture. In contrast, cardiac myocytes grow in three phases: a fetal period characterized by proliferative hyperplasia, a perinatal phase between birth and weaning that is characterized by hypertrophic growth and binucleation, and a third phase that spans weaning through adulthood, where myocytes grow primarily by hypertrophy. [89] The immediate postnatal period is a time of intense cardiac remodeling. [89,90] A study of sheep heart reported that right ventricle mass is greater than the left *in utero*. This imbalance was reversed in the weeks following birth as left ventricular cardiac myocytes grew larger. [90] A large scale analysis of rat cardiac DNA, RNA, and protein in the three stages of development also showed an oscillation of ventricular DNA in the perinatal period, with the highest recorded time point at PN7. [89] Given the role of Chd8 in regulating genes that correspond with cell growth and survival, the high levels of Chd8 mRNA expression observed at PN7 raise the possibility that elevated Chd8 protein plays a role in these transcriptional events.

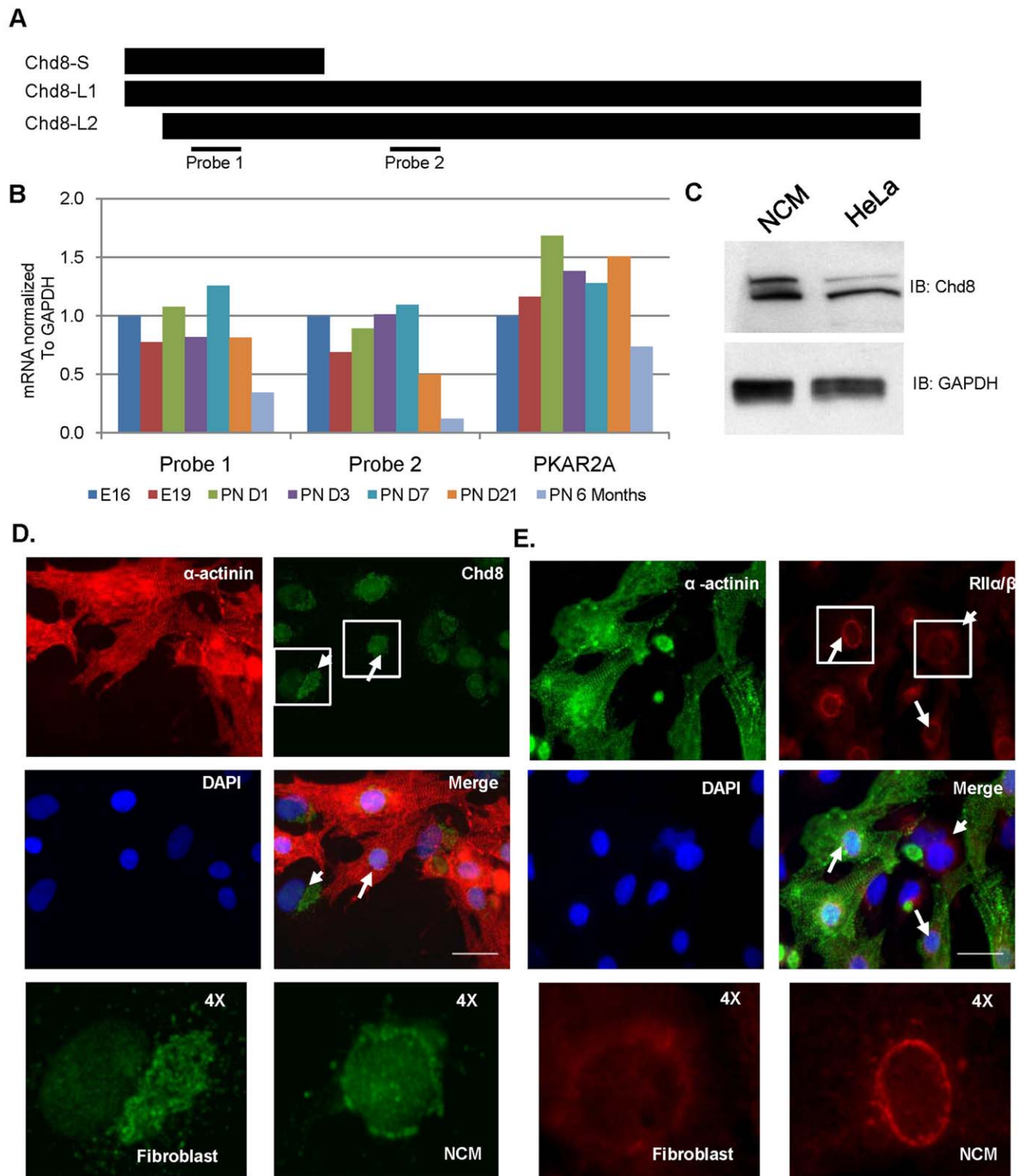


Figure 8. Expression and subcellular localization of Chd8 in cardiac development and in post-natal NCMs. A) A representation of the targets of the two sets of TaqMan probes used to measure Chd8 mRNA. Probe 1 (ABI IDRN00576005_m1) spans exon 2–3 and covers the RII binding domain. Probe 2 (ABI Rn01414467_m1) spans exons 12–13, which encode the helicase domain and detects only the two longest isoforms. B) Relative amounts of mRNA of Chd8 (Probe 1 and Probe 2) and RII α (PKAR2A), normalized to GAPDH and calculated by the $2^{-\Delta\Delta Ct}$ method. C) Western blot was used to detect Chd8-L1 and Chd8-L2 in NCMs. HeLa cell lysate was used as a positive control. D) NCMs were fixed at four days in culture and stained for Chd8 (green) and α -actinin (red). Arrows indicate myocytes, while arrowheads indicate fibroblasts. E) NCMs were fixed at four days in culture and stained for α -actinin (green) and RII α/β (red). Arrows indicate myocytes, while arrowheads indicate fibroblasts. Cells were imaged with inverted fluorescence microscopy and images taken at 90X magnification. Scale bar represents 25 μ m.

doi:10.1371/journal.pone.0046316.g008

Conclusions

In summary, we demonstrated that Chd8 contains an amino terminal RII α binding domain, between residues 455 and 473, and that this domain is required for RII α binding to Chd8. Immunofluorescence indicates a non-nuclear pool of Chd8 that appears to colocalize with RII and in proximity to markers against the Golgi apparatus. Nuclear and perinuclear microdomains of Chd8 were also identified in HeLa cells and in isolated rat NCMs. Moreover, dephosphorylation of RII α at Ser96 eliminates binding of RII α to Chd8-S, whereas RII α subunits pseudophosphorylated at Ser96 bind Chd8-S. These results indicate that Chd8 is a novel AKAP and demonstrate roles for Chd8 beyond its regulation of development, transcription, and cell survival.

Supporting Information

Figure S1 Negative control immunostaining with secondary antibodies in CHO and HeLa cells. A) CHO cells were incubated with Alexafluor Goat anti-Mouse 568 and imaged in conjunction with Chd8-S/Chd8-S-P transfections in Figure 4. Cells were imaged with inverted fluorescent microscopy at a magnification of 60X. Scale bar represents 38 μ m. B) HeLa cells were incubated with Alexafluor Goat anti-Rabbit 488 and Alexafluor Goat anti-Mouse 568 and imaged with inverted fluorescent microscopy at a magnification of 90X. Pane label indicates 488 or 568 channels. Scale bars represent 25 μ m. C) HeLa cells were incubated with Alexafluor Donkey anti-Goat 568 and Alexafluor Donkey anti-Mouse 488 and imaged with inverted fluorescent microscopy at a magnification of 90X. Scale bars represent 25 μ m. Pane label indicates 488 or 568 channels. D) HeLa cells were incubated with Alexafluor Donkey anti-Rabbit 568 and Alexafluor Donkey anti-Goat 488 and imaged with inverted fluorescent microscopy at a magnification of 90X. Scale bars represent 25 μ m. Pane label indicates 488 or 568 channels. (TIF)

Figure S2 Specificity of Chd8 and RII α / β antibodies in immunofluorescence. A) *Upper panels:* Unblocked immunofluorescence of Chd8. *Lower panels:* Immunofluorescence of endogenous Chd8 in HeLa cells with antibody preincubated for 1 hour with a three-fold excess of the peptide encompassing the antibody epitopes. Insets show immunofluorescence with secondary antibody (Alexafluor Donkey anti-Rabbit 568) alone. B) *Upper panels:* Unblocked immunofluorescence of RII α / β . *Lower panels:* Immunofluorescence of endogenous RII α / β in HeLa cells with antibody preincubated for 1 hour with a three-fold excess of purified recombinant RII α . Insets show immunofluorescence with secondary antibody (Alexafluor Donkey anti-Goat 488) alone. All cells

References

- Pidoux G, Tasken K (2010) Specificity and spatial dynamics of protein kinase A signaling organized by A-kinase-anchoring proteins. *J Mol Endocrinol* 44(5): 271–284. 10.1677/JME-10-0010.
- Scott JD, Stofko RE, McDonald JR, Comer JD, Vitalis EA, et al. (1990) Type II regulatory subunit dimerization determines the subcellular localization of the cAMP-dependent protein kinase. *J Biol Chem* 265(35): 21561–6.
- Diviani D, Dodge Kafka K, Li J, Kapiloff M (2011) A-kinase anchoring proteins: Scaffolding proteins in the heart. *American Journal of Physiology, Heart and Circulatory Physiology* 301(5): H1742–H1753. 10.1152/ajpheart.00569.2011.
- Greenwald E, Saucerman J (2011) Bigger, better, faster: Principles and models of AKAP anchoring protein signaling. *J Cardiovasc Pharmacol* 58(5): 462–469. 10.1097/FJC.0b013e31822001e3.
- Mauban JR, O'Donnell M, Warrior S, Manni S, Bond M (2009) AKAP-scaffolding proteins and regulation of cardiac physiology. *Physiology (Bethesda)* 24: 78–87.
- Scott JD, McCartney S (1994) Localization of A-kinase through anchoring proteins. *Molecular Endocrinology* 8(1): 5–11. 10.1210/me.8.1.5.
- Skroblin P, Grossmann S, Schfer G, Rosenthal W, Klusmann E (2010) Mechanisms of protein kinase A anchoring. *Int Rev Cell Mol Biol* 283: 235–330. 10.1016/S1937-6448(10)83005-9.
- Nicolas CS, Park KH, El Harchi A, Camonis J, Kass RS, et al. (2008) IKs response to protein kinase A-dependent KCNQ1 phosphorylation requires direct interaction with microtubules. *Cardiovasc Res*.
- Chen L, Marquardt ML, Tester DJ, Sampson KJ, Ackerman MJ, et al. (2007) Mutation of an A-kinase-anchoring protein causes long-QT syndrome. *Proc Natl Acad Sci U S A* 104(52): 20990–5.
- Chen L, Kurokawa J, Kass RS (2005) Phosphorylation of the A-kinase-anchoring protein yotiao contributes to protein kinase A regulation of a heart potassium channel. *J Biol Chem* 280(36): 31347–52.
- Kurokawa J, Motoike HK, Rao J, Kass RS (2004) Regulatory actions of the A-kinase anchoring protein yotiao on a heart potassium channel downstream of PKA phosphorylation. *Proc Natl Acad Sci U S A* 101(46): 16374–8.
- Carnegie G, Soughayer J, Smith FD, Pedroja B, Zhang F, et al. (2008) AKAP-lbc mobilizes a cardiac hypertrophy signaling pathway. *Mol Cell* 32(2): 169–179. 10.1016/j.molcel.2008.08.030.

were imaged with inverted fluorescent microscopy at a magnification of 90X. Scale bars represent 25 μ m. (TIF)

Figure S3 Negative control immunostaining with secondary antibodies in NCMs. A) Isolated rat cardiac cells were incubated with Alexafluor Goat anti-Mouse 568 and Alexafluor Goat anti-Rabbit 488 and imaged with inverted fluorescent microscopy at a magnification of 90X. B) Isolated rat cardiac cells were incubated with Alexafluor Donkey anti-Goat 568 and Alexafluor Donkey anti-Mouse 488 and imaged with inverted fluorescent microscopy at a magnification of 90X. Scale bars represent 25 μ m. (TIF)

Figure S4 Immunofluorescence of HeLa cells and NCM with an alternate Chd8 antibody. A) *Top Row:* HeLa cells were incubated with Chd8-Sigma antibody and Alexafluor Goat anti-Rabbit 488, and imaged with inverted fluorescent microscopy. *Bottom Row:* HeLa cells were incubated with secondary antibody alone. Scale bars represent 25 μ m. B) NCMs were fixed at four days in culture and stained for α -actinin (red) and Chd8-Sigma (green), detected with Alexafluor Goat anti-mouse 568 and Alexafluor Goat anti-rabbit 488, respectively. Short arrows indicate myocytes, while long arrows indicate fibroblasts. Cells were imaged with inverted fluorescence microscopy. Scale bar represents 25 μ m. (TIF)

Table S1 Prediction of phosphorylation sites on the amino terminus of Chd8. The prediction program PKAps was used to generate predictions of PKA phosphorylation targets in the first 800 amino acids of Chd8 [88]. Phosphorylation sites that occur within a known domain of Chd8 are marked. Phosphorylation sites that fall within regions. The phosphorylated residue is bolded and underlined. (DOC)

Acknowledgments

We would like to thank Dr. Akira Kikuchi (Hiroshima University, Japan) for the gift of the rat Chd8-S plasmid, and Yinghua Zhang (University of Maryland, Baltimore) for the cardiac embryonic timecourse tissue.

Author Contributions

Conceived and designed the experiments: MOS LL SM MR JM MB. Performed the experiments: MOS LL SM MR JM. Analyzed the data: MOS JM. Contributed reagents/materials/analysis tools: MOS SM MR JM MB. Wrote the paper: MOS LL MB. Editing: MOS LL MB.

13. Dodge-Kafka KL, Soughayer J, Pare GC, Carlisle Michel JJ, Langeberg LK, et al. (2005) The protein kinase A anchoring protein mAKAP coordinates two integrated cAMP effector pathways. *Nature* 437(7058): 574–8.
14. Appert Collin A, Cotecchia S, Nenniger Tosato M, Pedrazzini T, Diviani D (2007) The A-kinase anchoring protein (AKAP)-Ibc-signaling complex mediates alpha1 adrenergic receptor-induced cardiomyocyte hypertrophy. *Proc Natl Acad Sci U S A* 104(24): 10140–10145. 10.1073/pnas.0701099104.
15. Zakhary DR, Moravec CS, Bond M (2000) Regulation of PKA binding to AKAPs in the heart: Alterations in human heart failure. *Circulation* 101(12): 1459–64.
16. Ruehr ML, Russell MA, Bond M (2004) A-kinase anchoring protein targeting of protein kinase A in the heart. *J Mol Cell Cardiol* 37(3): 653–65.
17. Fink MA, Zakhary DR, Mackey JA, Desnoyer RW, Apperson-Hansen C, et al. (2001) AKAP-mediated targeting of protein kinase A regulates contractility in cardiac myocytes. *Circ Res* 88(3): 291–7.
18. Aye T, Soni S, van Veen TAB, van der Heyden, Marcel AG, et al. (2012) Reorganized PKA-AKAP associations in the failing human heart. *J Mol Cell Cardiol* 52(2): 511–518. 10.1016/j.yjmcc.2011.06.003.
19. Zakhary DR, Fink MA, Ruehr ML, Bond M (2000) Selectivity and regulation of A-kinase anchoring proteins in the heart. the role of autophosphorylation of the type II regulatory subunit of cAMP-dependent protein kinase. *J Biol Chem* 275(52): 41389–95.
20. Manni S, Mauban JH, Ward CW, Bond M (2008) Phosphorylation of the cAMP-dependent protein kinase (PKA) regulatory subunit modulates PKA-AKAP interaction, substrate phosphorylation, and calcium signaling in cardiac cells. *J Biol Chem* 283(35): 24145–54.
21. Pandya K, Pulli B, Bultman S, Smithies O (2010) Reversible epigenetic modifications of the two cardiac myosin heavy chain genes during changes in expression. *Gene Expr* 15(2): 51–59. 10.3727/105221611X12973615737505.
22. Miyata S, Minobe W, Bristow MR, Leinwand LA (2000) Myosin heavy chain isoform expression in the failing and nonfailing human heart. *Circ Res* 86(4): 386–390.
23. Rajabi M, Kassiotis C, Razeghi P, Taegtmeyer H (2007) Return to the fetal gene program protects the stressed heart: A strong hypothesis. *Heart Fail Rev* 12(3–4): 331–43.
24. Carr DW, Stofko-Hahn RE, Fraser ID, Bishop SM, Acott TS, et al. (1991) Interaction of the regulatory subunit (RII) of cAMP-dependent protein kinase with RII-anchoring proteins occurs through an amphipathic helix binding motif. *J Biol Chem* 266(22): 14188–92.
25. Carr DW, Hausken ZE, Fraser ID, Stofko-Hahn RE, Scott JD (1992) Association of the type II cAMP-dependent protein kinase with a human thyroid RII-anchoring protein. cloning and characterization of the RII-binding domain. *J Biol Chem* 267(19): 13376–82.
26. Vijayaraghavan S, Liberty GA, Mohan J, Winfrey VP, Olson GE, et al. (1999) Isolation and molecular characterization of AKAP110, a novel, sperm-specific protein kinase A-anchoring protein. *Mol Endocrinol* 13(5): 705–17.
27. Russell MA, Lund LM, Haber R, McKeegan K, Cianciola N, et al. (2006) The intermediate filament protein, synemin, is an AKAP in the heart. *Arch Biochem Biophys*.
28. Yamashina K, Yamamoto H, Chayama K, Nakajima K, Kikuchi A (2006) Suppression of STAT3 activity by duplin, which is a negative regulator of the wnt signal. *J Biochem* 139(2): 305–314. 10.1093/jb/mvj033.
29. Ishihara K, Oshimura M, Nakao M (2006) CTCF-dependent chromatin insulator is linked to epigenetic remodeling. *Mol Cell* 23(5): 733–742. 10.1016/j.molcel.2006.08.008.
30. Yates JA, Menon T, Thompson BA, Bochar DA (2010) Regulation of HOXA2 gene expression by the ATP-dependent chromatin remodeling enzyme CHD8. *FEBS Lett* 584(4): 689–693. 10.1016/j.febslet.2010.01.022.
31. Thompson BA, Tremblay V, Lin G, Bochar DA (2008) CHD8 is an ATP-dependent chromatin remodeling factor that regulates beta-catenin target genes. *Mol Cell Biol* 28(12): 3894–3904. 10.1128/MCB.00322–08.
32. Rodriguez-Paredes M, Ceballos-Chavez M, Esteller M, Garcia-Dominguez M, Reyes JC (2009) The chromatin remodeling factor CHD8 interacts with clonating RNA polymerase II and controls expression of the cyclin E2 gene. *Nucleic Acids Res* 37(8): 2449–2460. 10.1093/nar/gkp101.
33. Yuan CC, Zhao X, Florens L, Swanson SK, Washburn MP, et al. (2007) CHD8 associates with human *staf* and contributes to efficient U6 RNA polymerase III transcription. *Mol Cell Biol* 27(24): 8729–8738. 10.1128/MCB.00846–07.
34. Rodenberg JM, Hoggatt AM, Chen M, Touw K, Jones RE, et al. (2010) Regulation of serum response factor activity and smooth muscle cell apoptosis by chromodomain helicase dna-binding protein 8. *Am J Physiol Cell Physiol*. 10.1152/ajpcell.00080.2010.
35. Nishiyama M, Skoultschi A, Nakayama K (2012) Histone H1 recruitment by CHD8 is essential for suppression of the wnt- β -catenin signaling pathway. *Mol Cell Biol* 32(2): 501–512. 10.1128/MCB.06409–11.
36. Nishiyama M, Oshikawa K, Tsukada Y, Nakagawa T, Iemura S, et al. (2009) CHD8 suppresses p53-mediated apoptosis through histone H1 recruitment during early embryogenesis. *Nat Cell Biol* 11(2): 172–182. 10.1038/ncb1831.
37. Sakamoto I, Kishida S, Fukui A, Kishida M, Yamamoto H, et al. (2000) A novel beta-catenin-binding protein inhibits beta-catenin-dependent *tcf* activation and axis formation. *J Biol Chem* 275(42): 32871–32878. 10.1074/jbc.M004089200.
38. Kobayashi M, Kishida S, Fukui A, Michiue T, Miyamoto Y, et al. (2002) Nuclear localization of duplin, a beta-catenin-binding protein, is essential for its inhibitory activity on the wnt signaling pathway. *J Biol Chem* 277(8): 5816–5822. 10.1074/jbc.M108433200.
39. Nishiyama M, Nakayama K, Tsunematsu R, Tsukiyama T, Kikuchi A, et al. (2004) Early embryonic death in mice lacking the beta-catenin-binding protein duplin. *Mol Cell Biol* 24(19): 8386–8394. 10.1128/MCB.24.19.8386–8394.2004.
40. Menon T, Yates JA, Bochar DA (2010) Regulation of androgen-responsive transcription by the chromatin remodeling factor CHD8. *Mol Endocrinol* 24(6): 1165–1174. 10.1210/me.2009-0421.
41. Sample V, Dipilato L, Yang J, Ni Q, Saucerman J, et al. (2012) Regulation of nuclear PKA revealed by spatiotemporal manipulation of cyclic AMP. *Nature Chemical Biology* 8(4): 375–382. 10.1038/nchembio.799.
42. Zippin J, Farrell J, Huron D, Kamenetsky M, Hess K, et al. (2004) Bicarbonate-responsive “soluble” adenylyl cyclase defines a nuclear cAMP microdomain. *J Cell Biol* 164(4): 527–534. 10.1083/jcb.200311119.
43. Wright G, Singh I, Hasday J, Farrance I, Hall G, et al. (2002) Endotoxin stress-response in cardiomyocytes: NF-kappaB activation and tumor necrosis factor-alpha expression. *American Journal of Physiology. Heart and Circulatory Physiology* 282(3): H872–H879. 10.1152/ajpheart.00256.2001.
44. Lund L, Kerr J, Lupinetti J, Zhang Y, Russell M, et al. (2012) Synemin isoforms differentially organize cell junctions and desmin filaments in neonatal cardiomyocytes. *FASEB Journal* 26(1): 137.
45. Schmitgen T, Livak K (2008) Analyzing real-time PCR data by the comparative C(T) method. *Nature Protocols* 3(6): 1101–1108. 10.1038/nprot.2008.73.
46. Lohmann SM, DeCamilli P, Einig I, Walter U (1984) High-affinity binding of the regulatory subunit (RII) of cAMP-dependent protein kinase to microtubule-associated and other cellular proteins. *Proc Natl Acad Sci U S A* 81(21): 6723–6727. 10.1073/pnas.81.21.6723.
47. Kapiloff MS, Schillace RV, Westphal AM, Scott JD (1999) mAKAP: An A-kinase anchoring protein targeted to the nuclear membrane of differentiated myocytes. *J Cell Sci* 112(16): 2725–2736.
48. Diviani D, Soderling J, Scott JD (2001) AKAP-Ibc anchors protein kinase A and nucleates galpha 12-selective rho-mediated stress fiber formation. *J Biol Chem* 276(47): 44247–44257. 10.1074/jbc.M106629200.
49. Garnier J, Gibrat JF, Robson B (1996) GOR method for predicting protein secondary structure from amino acid sequence. *Meth Enzymol* 266: 540–553. 10.1016/S0076-6879(96)66034-0.
50. Robson B, Pain RH (1974) Analysis of the code relating sequence to conformation in globular proteins. an informational analysis of the role of the residue in determining the conformation of its neighbours in the primary sequence. *Biochem J* 141(3): 883–897.
51. Cole C, Barber J, Barton G (2008) The jpred 3 secondary structure prediction server. *Nucleic Acids Res* 36(Web Server issue): W197–W201. 10.1093/nar/gkn238.
52. Larkin MA, Blackshields G, Brown NP, Chenna R, McGettigan PA, et al. (2007) Clustal W and clustal X version 2.0. *Bioinformatics* 23(21): 2947–2948. 10.1093/bioinformatics/btm404.
53. Fischer DK (1996) Helical wheel custom images and interactive java applet.
54. Carr DW, Scott JD (1992) Blotting and band-shifting: Techniques for studying protein-protein interactions. *Trends Biochem Sci* 17(7): 246–9.
55. Carr DW, Stofko-Hahn RE, Fraser ID, Cone RD, Scott JD (1992) Localization of the cAMP-dependent protein kinase to the postsynaptic densities by A-kinase anchoring proteins. characterization of AKAP 79. *J Biol Chem* 267(24): 16816–23.
56. Hausken ZE, Coghlan VM, Hastings CA, Reimann EM, Scott JD (1994) Type II regulatory subunit (RII) of the cAMP-dependent protein kinase interaction with A-kinase anchor proteins requires isoleucines 3 and 5. *J Biol Chem* 269(39): 24245–51.
57. Herberg FW, Maleszka A, Eide T, Vossebein L, Tasken K (2000) Analysis of A-kinase anchoring protein (AKAP) interaction with protein kinase A (PKA) regulatory subunits: PKA isoform specificity in AKAP binding. *J Mol Biol* 298(2): 329–39.
58. Alto NM, Soderling SH, Hoshi N, Langeberg LK, Fayos R, et al. (2003) Bioinformatic design of A-kinase anchoring protein-in silico: A potent and selective peptide antagonist of type II protein kinase A anchoring. *Proc Natl Acad Sci U S A* 100(8): 4445–50.
59. Taylor SS, Buechler JA, Yonemoto W (1990) cAMP-dependent protein kinase: Framework for a diverse family of regulatory enzymes. *Annu Rev Biochem* 59: 971–1005. 10.1146/annurev.bi.59.070190.004543.
60. Taskn K, Aandahl E (2004) Localized effects of cAMP mediated by distinct routes of protein kinase A. *Physiol Rev* 84(1): 137–167. 10.1152/physrev.00021.2003.
61. Erlichman J, Rosenfeld R, Rosen OM (1974) Phosphorylation of a cyclic adenosine 3′: 5′-monophosphate-dependent protein kinase from bovine cardiac muscle. *J Biol Chem* 249(15): 5000–5003.
62. Shanks R, Steadman B, Schmidt PH, Goldring J (2002) AKAP350 at the golgi apparatus. I. identification of a distinct golgi apparatus targeting motif in AKAP350. *J Biol Chem* 277(43): 40967–40972. 10.1074/jbc.M203307200.
63. Rogers R, Norian J, Malik M, Christman G, Abu Asab M, et al. (2008) Mechanical homeostasis is altered in uterine leiomyoma. *Obstet Gynecol* 198(4): 474.e1–474.11. 10.1016/j.ajog.2007.11.057.
64. Mayers C, Wadell J, McLean K, Venero M, Malik M, et al. (2010) The rho guanine nucleotide exchange factor AKAP13 (BRX) is essential for cardiac development in mice. *J Biol Chem* 285(16): 12344–12354. 10.1074/jbc.M110.106856.

65. McLaughlin W, Hou T, Taylor S, Wang W (2011) The identification of novel cyclic AMP-dependent protein kinase anchoring proteins using bioinformatic filters and peptide arrays. *Protein Engineering, Design Selection* 24(3): 333–339. 10.1093/protein/gzq106.
66. Means C, Lygren B, Langeberg L, Jain A, Dixon R, et al. (2011) An entirely specific type I A-kinase anchoring protein that can sequester two molecules of protein kinase A at mitochondria. *Proc Natl Acad Sci U S A* 108(48): E1227–E1235. 10.1073/pnas.1107182108.
67. Landsverk HB, Carlson CR, Steen RL, Vossebein L, Herberg FW, et al. (2001) Regulation of anchoring of the RIIalpha regulatory subunit of PKA to AKAP95 by threonine phosphorylation of RIIalpha: Implications for chromosome dynamics at mitosis. *J Cell Sci* 114(Pt 18): 3255–64.
68. Dodge-Kafka KL, Langeberg L, Scott JD (2006) Compartmentation of cyclic nucleotide signaling in the heart: The role of A-kinase anchoring proteins. *Circ Res* 98(8): 993–1001.
69. Zippin J, Chen Y, Nahirney P, Kamenetsky M, Wuttke M, et al. (2003) Compartmentalization of bicarbonate-sensitive adenylyl cyclase in distinct signaling microdomains. *The FASEB Journal* 17(1): 82–84. 10.1096/fj.02-0598jfe.
70. Patel H, Hamuro L, Chun B, Kawaraguchi Y, Quick A, et al. (2010) Disruption of protein kinase A localization using a trans-activator of transcription (TAT)-conjugated A-kinase-anchoring peptide reduces cardiac function. *J Biol Chem* 285(36): 27632–27640. 10.1074/jbc.M110.146589.
71. Roth J, Bendayan M, Orci L (1978) Ultrastructural localization of intracellular antigens by the use of protein A-gold complex. *J Histochem Cytochem* 26(12): 1074–81.
72. Miller P, Walter U, Theurkauf WE, Vallee RB, De Camilli P (1982) Frozen tissue sections as an experimental system to reveal specific binding sites for the regulatory subunit of type II cAMP-dependent protein kinase in neurons. *Proc Natl Acad Sci U S A* 79(18): 5562–6.
73. Mednieks MI, Jungmann RA, Fischler C, Hand AR (1989) Immunogold localization of the type II regulatory subunit of cyclic AMP-dependent protein kinase. monoclonal antibody characterization and RII distribution in rat parotid cells. *J. Histochem. Cytochem.* 37(3): 339–346.
74. Zippin J, Chadwick P, Levin L, Buck J, Magro C (2010) Soluble adenylyl cyclase defines a nuclear cAMP microdomain in keratinocyte hyperproliferative skin diseases. *J Invest Dermatol* 130(5): 1279–1287. 10.1038/jid.2009.440.
75. Chen J, Levin L, Buck J (2012) Role of soluble adenylyl cyclase in the heart. *American Journal of Physiology. Heart and Circulatory Physiology* 302(3): H538–H543. 10.1152/ajpheart.00701.2011.
76. Zhang Q, Carr DW, Lerea KM, Scott JD, Newman SA (1996) Nuclear localization of type II cAMP-dependent protein kinase during limb cartilage differentiation is associated with a novel developmentally regulated A-kinase anchoring protein. *Dev Biol* 176(1): 51–61.
77. Shmyrev II, Grozdova ID, Kondratyev AD, Mamayeva EG, Severin ES (1990) Immunofluorescence localization of the regulatory subunit type II of cAMP-dependent protein kinase in PC12 and 3T3 cells in different proliferative states. *Mol Cell Biochem* 93(1): 47–52. 10.1007/BF00223491.
78. Trinczek B, Robert-Nicoud M, Schwoch G (1993) In situ localization of cAMP-dependent protein kinases in nuclear and chromosomal substructures: Relation to transcriptional activity. *Eur J Cell Biol* 60(1): 196–202.
79. Squinto SP, Jungmann RA (1989) Modulation of nuclear cyclic AMP-dependent protein kinase in dibutyl cyclic AMP-treated rat H4IIE hepatoma cells. *Biochem J* 260(3): 673–82.
80. Eide T, Carlson C, Tasken KA, Hirano T, Tasken K, et al. (2002) Distinct but overlapping domains of AKAP95 are implicated in chromosome condensation and condensin targeting. *EMBO Rep* 3(5): 426–32.
81. Collas P, Le Guellec K, Tasken K (1999) The A-kinase-anchoring protein AKAP95 is a multivalent protein with a key role in chromatin condensation at mitosis. *J Cell Biol* 147(6): 1167–80.
82. Eide T, Coghlan V, Orstavik S, Holsve C, Solberg R, et al. (1998) Molecular cloning, chromosomal localization, and cell cycle-dependent subcellular distribution of the A-kinase anchoring protein, AKAP95. *Exp Cell Res* 238(2): 305–16.
83. Brown RL, August SL, Williams CJ, Moss SB (2003) AKAP7gamma is a nuclear RI-binding AKAP. *Biochem Biophys Res Commun* 306(2): 394–401.
84. Jarnaess E, Stokka A, Kvissel A, Sklhegg B, Torgersen K, et al. (2009) Splicing factor arginine/serine-rich 17A (SFRS17A) is an A-kinase anchoring protein that targets protein kinase A to splicing factor compartments. *J Biol Chem* 284(50): 35154–35164. 10.1074/jbc.M109.056465.
85. Smyth J, Vogan J, Buch P, Zhang S, Fong T, et al. (2012) Actin cytoskeleton rest stops regulate anterograde traffic of connexin 43 vesicles to the plasma membrane. *Circ Res* 110(7): 978–989. 10.1161/CIRCRESAHA.111.257964.
86. Scholten A, van Veen TAB, Vos M, Heck AJR (2007) Diversity of cAMP-dependent protein kinase isoforms and their anchoring proteins in mouse ventricular tissue. *Journal of Proteome Research* 6(5): 1705–1717. 10.1021/pr060601a.
87. Zhang F, White RL, Neufeld KL (2000) Phosphorylation near nuclear localization signal regulates nuclear import of adenomatous polyposis coli protein. *Proc Natl Acad Sci U S A* 97(23): 12577–12582. 10.1073/pnas.230435597.
88. Neuberger G, Schneider G, Eisenhaber F (2007) pkaPS: Prediction of protein kinase A phosphorylation sites with the simplified kinase-substrate binding model. *Biology Direct* 2: 1–1. 10.1186/1745-6150-2-1.
89. van den Hoff MJ, Deprez RH, Monteiro M, de Boer PA, Charles R, et al. (1997) Developmental changes in rat cardiac DNA, RNA and protein tissue base: Implications for the interpretation of changes in gene expression. *J Mol Cell Cardiol* 29(2): 629–639. 10.1006/jmcc.1996.0306.
90. Smolich JJ (1995) Ultrastructural and functional features of the developing mammalian heart: A brief overview. *Reproduction, Fertility and Development* 7(3): 451–461. 10.1071/RD9950451.
91. Marfella CG, Imbalzano AN (2007) The chd family of chromatin remodelers. *Mutat Res* 618(1–2): 30–40.
92. Hall JA, Georgel P (2007) CHD proteins: A diverse family with strong ties. *Biochemistry and Cell Biology* 85(4): 463–476. 10.1139/O07-063.